European Polymer Journal 47 (2011) 1686–1693

Contents lists available at ScienceDirect

European Polymer Journal

journal homepage: www.elsevier.com/locate/europolj

Synthesis and investigation of photovoltaic properties for polymer semiconductors based on porphyrin compounds as light-harvesting units

Jang Yong Lee [a], Ho Jun Song [a], Seung Min Lee [a], Jun Hee Lee [b], Doo Kyung Moon [a,*]

[a] Department of Materials Chemistry and Engineering, Konkuk University, 1 Hwayang-dong, Gwangjin-gu, Seoul 143-701, Republic of Korea
[b] Department of Materials Science and Engineering, Dong-A University, Hadan2-dong, Saha-gu, Busan 604-714, Republic of Korea

ARTICLE INFO

Article history:
Received 20 April 2011
Received in revised form 3 June 2011
Accepted 7 June 2011
Available online 11 July 2011

Keywords:
Porphyrin compound
Conjugated polymers
Copolymerization
Organic photovoltaics

ABSTRACT

We reported on two polymer semiconducting copolymers based on porphyrin compounds, poly[9,9-dioctylfluorene-co-5,15-bis(hexoxybenzyl)-10,20-bis(benzo-4-yl)porphyrin] (PFPor) and poly[9-(heptadecan-9-yl)carbazole-co-5,15-bis(hexoxybenzyl)-10,20-bis(benzo-4-yl)porphyrin] (PCPor), for use as organic photovoltaic materials. The thermal, optical, electrochemical, and photovoltaic properties of the two polymers were investigated. In addition, $PC_{61}BM$ and $PC_{71}BM$ were introduced as acceptor materials to confirm the acceptor effect in bulk heterojunction photovoltaic devices. Moreover, in order to establish acceptor effects, morphologies of polymer/PCBM blend films were analyzed through atomic force microscopy (AFM). PFPor and PCPor exhibited the best device performance with power conversion efficiencies (PCE) of 0.62% and 0.76%, respectively, upon the introduction of $PC_{71}BM$ as the acceptor in the device where 86 wt.% of the $PC_{71}BM$ was contained in the active layer (pol:$PC_{71}BM$ = 1:6, w/w).

1. Introduction

Polymer solar cell has been vigorously investigated for several decades due to various advantages, such as low-cost, flexibility, eco-friendly use, etc. Recently, developments of fabrication technologies of flexible and large area devices, such as ink-jet printing and roll-to-roll through solution processing [1–5], have increased the practical potential of organic solar cells (OPVs) towards next generation energy converting devices. Due to intensive research into organic semiconducting polymers, outstanding photovoltaic materials have been developed [6–12]. In order to improve the PCEs of photovoltaic devices it is the most important to design and synthesize polymer materials that exhibit a broad absorption of the solar spectrum, a planar molecular structure, a good stacking property between molecules and good charge transport properties, etc. [13,14]. In this sense, porphyrin derivatives have been regarded as promising candidate for photovoltaic materials due to their various optical and excellent charge transporting properties due to their good planarity and flat formations [15–19].

Porphyrin derivatives have highly light-sensitive dye molecules which play important roles in natural photosynthetic systems as light-harvesting antenna components for the efficient capture of visible photons [20–22]. Additionally, since they exhibited a strong absorption spectrum over 600 nm due to a strong Q-band absorption region, porphyrin derivatives have been regarded as outstanding candidates in organic photovoltaics, such as polymer solar cells and dye sensitized solar cells [23,24].

In this study, two photovoltaic polymer materials based on porphyrin, PFPor and PCPor, were demonstrated. In order to reinforce the open circuit voltage (V_{OC}) values of porphyrin-based materials, fluorene or carbazole that had low highest occupied molecular orbital (HOMO) energy levels were introduced into the polymer skeleton [25]. Bulk heterojunction-type devices that utilized 1-(3-methoxycarbonyl)propyl-1-phenyl-6,6-C-61 ($PC_{61}BM$) and

* Corresponding author. Tel.: +82 2 450 3498; fax: +82 2 444 0765.
E-mail address: dkmoon@konkuk.ac.kr (D.K. Moon).

0014-3057/$ - see front matter © 2011 Elsevier Ltd. All rights reserved.
doi:10.1016/j.eurpolymj.2011.06.005

1-(3-methoxycarbonyl)propyl-1-phenyl-6,6-C-71 ($PC_{71}BM$) as acceptors were fabricated in order to investigate the photovoltaic properties of PFPor and PCPor.

2. Experimental methods

2.1. Instruments and characterization

All of the reagents and chemicals were purchased from Aldrich and used as received unless otherwise specified. The ^1H NMR (400 MHz) spectra were recorded using a Brüker AMX400 spectrometer in $CDCl_3$, and the chemical shifts were recorded in units of ppm with TMS as the internal standard. The elemental analyses were measured with EA1112 using a CE Instrument. Since their molecular weights and number of molecules were too small compared to those of polymer chains, end-capping molecules were not considered in calculated elemental analyses data. The absorption spectra were recorded using an Agilent 8453 UV–Visible spectroscopy system. The solutions that were used for the UV–Visible and photoluminescense (PL) spectroscopy measurements were dissolved in chloroform. The films were drop-coated from the chloroform solution onto a quartz substrate. All of the GPC analyses were carried out using THF as the eluent and a polystyrene standard as the reference. The TGA measurements were performed using a TA Instrument 2050. The decomposition temperature (T_d) was determined as a point where 5% weight loss was shown. The cyclic voltammetric waves were produced using a Zahner IM6eX electrochemical workstation with a 0.1 M acetonitrile (substituted with nitrogen for 20 min) solution containing tetrabutyl ammonium hexafluorophosphate (Bu_4NPF_6) as the electrolyte at a constant scan rate of 50 mV/s. ITO, a Pt wire, and silver/silver chloride [Ag in 0.1 M KCl] were used as the working, counter, and reference electrodes, respectively. The electrochemical potential was calibrated against Fc/Fc^+. The HOMO levels of the polymers were determined using the oxidation onset value. Onset potentials are values obtained from the intersection of the two tangents drawn at the rising current and the baseline changing current of the CV curves. The LUMO levels were calculated from the differences between the HOMO energy levels and the optical band-gaps, which were determined using the UV–Vis absorption onset values in the films.

The current–voltage (I–V) curves of the photovoltaic devices were measured using a computer-controlled Keithley 2400 source measurement unit (SMU) that was equipped with a Peccell solar simulator under an illumination of AM 1.5 G (100 mW/cm^2). Thicknesses of the thin films were measured using a KLA Tencor Alpha-step 500 surface profilometer with an accuracy of 1 nm. Topographic images of the active layers were obtained through AFM in tapping mode under ambient conditions using a XE-100 instrument.

2.2. Fabrication and characterization of polymer solar cells

All of the bulk-heterojunction PV cells were prepared using the following device fabrication procedure. The glass/indium tin oxide (ITO) substrates [Sanyo, Japan (10 Ω/γ)] were sequentially lithographically patterned, cleaned with detergent, and ultrasonicated in deionized water, acetone, and isopropyl alcohol. Then the substrates were dried on a hot-plate at 120 °C for 10 min and treated with oxygen plasma for 10 min in order to improve the contact angle just before the film coating process. Poly(3,4-ethylene-dioxythiophene): poly(styrene-sulfonate) (PEDOT:PSS, Baytron P 4083 Bayer AG) was passed through a 0.45 μm filter before being deposited onto ITO at a thickness of ca. 32 nm by spin-coating at 4000 rpm in air and then it was dried at 120 °C for 20 min inside a glove box. Composite solutions with polymers and PCBM were prepared using 1,2-dichlorobenzene (DCB). The concentration was controlled adequately in the 0.5 wt.% range, and the solutions were then filtered through a 0.45 μm PTFE filter and then spin-coated on top of the PEDOT:PSS layer. The device fabrication was completed by depositing thin layers of BaF_2 (1 nm), Ba (2 nm), and Al (200 nm) at pressures of less than 10^{-6} torr. The active area of the device was 4.0 mm^2. Finally, the cell was encapsulated using UV-curing glue (Nagase, Japan). In this study, all of the devices were fabricated with the following structure: ITO glass/PEDOT:PSS/polymer:PCBM/BaF_2/Ba/Al/encapsulation glass.

The illumination intensity was calibrated using a standard a Si photodiode detector that was equipped with a KG-5filter. The output photocurrent was adjusted to match the photocurrent of the Si reference cell in order to obtain a power density of 100 mW/cm^2. After the encapsulation, all of the devices were operated under an ambient atmosphere at 25 °C.

2.3. Materials

All reagents were purchased from Aldrich, Acros or TCI companies. All chemicals were used without further purification. The following compounds were synthesized following modified literature procedures: 2,2′-(9,9-dioctyl-9H-fluorene-2,7-diyl)bis(4,4,5,5-tetramethyl-1,3,2-dioxaborolane) **4** [26], 9-(heptadecan-9-yl)-2,7-bis(4,4,5,5-tetramethyl-1,3, 2- dioxaborolan-2-yl)-9H-carbazole **5** [27].

2.3.1. 4-(Hexyloxy)benzaldehyde (1)

4-hydroxybenzaldehyde (5 g, 40.94 mmol), K_2CO_3 (8.48 g, 61.41 mmol), and *N*,*N*-dimethylformamide (DMF) (50 mL) were placed in a 250 ml two-neck round-bottom flask, and then, this mixture was stirred at 50 °C for 1 h. Then 1-bromohexane (8.11 g, 49.12 mmol) was dropped into the mixture and stirred at 90 °C for 48 h. The reaction mixture was extracted using chloroform/brine, and then, the organic layer was separated and concentrated. The product was purified using column chromatography using dichloromethane as the eluent. The product yield was 93% (7.93 g). ^1H NMR (400 MHz; $CDCl_3$; Me_4Si): 9.85 (s, 1H), 7.80 (d, 2H), 6.97 (d, 2H), 4.01 (t, 2H), 1.80 (m, 2H), 1.44 (m, 2H), 1.33 (m, 4H), 0.90 (t, 3H). ^{13}C NMR (100 MHz; $CDCl_3$; Me_4Si): 190.71, 164.22, 131.95, 129.66, 114.68, 68.35, 31.52, 29.17, 25.83, 22.58, 14.03.

2.3.2. 2,2′-((4-Bromophenyl)methylene)bis(2,5-dihydro-1H-pyrrole) ***(2)***

4-Bromobenzaldehyde (3 g, 16.21 mmol) and pyrrole (43.50 g, 648.4 mmol) were placed in a 250 mL two-neck round bottom flask, and then this mixture was stirred for 10 min at room temperature. Trifluoroacetic acid (0.184 g, 1.62 mmol) was added to the reaction mixture and stirred for 90 min. The reaction mixture was treated with NaOH (1.94 g, 48.63 mmol), and then the mixture was stirred for 45 min. After filtration, excess pyrrole was concentrated in vacuo. The product was purified using column chromatography using EA, MC, Hex (1:2:7) as the eluent. The product yield was 62% (3.1 g). ^{1}H NMR (400 MHz; $CDCl_3$; Me_4Si): 7.89 (s, 2H), 7.47 (d, 2H), 7.11 (d, 2H), 6.72 (d, 2H), 6.21 (d, 2H), 5.93 (br s, 2H), 5.42 (s, 1H). ^{13}C NMR (100 MHz; $CDCl_3$; Me_4Si): 141.2, 131.7, 131.9, 130.2, 120.9, 117.6, 108.6, 107.5, 43.4. Elem. Anal. for $C_{14}H_{15}N_2Br$ Calc.: C, 59.42; H, 4.99; N, 9.26. Found: C, 59.18; H, 4.30; N, 9.15.

2.3.3. 5,15-Bis(hexoxybenzyl)-10,20-bis(4-bromobenzyl)porphyrin ***(3)***

Compound **1** (2.02 g, 9.82 mmol), **2** (3 g, 9.82 mmol) and dichloromethane (982 ml) were placed in a 2000 mL two-neck round-bottom flask, and then they were bubbled for 30 min under nitrogen. After bubbling, trifluoroacetic acid (1.11 g, 9.82 mmol) was added into the mixture and stirred for 90 min., and then *p*-chroranil was added into the mixture and stirred for 1 h. The reaction mixture was treated with TEA (1.49 g, 14.73 mmol). Then zinc acetate (2.05 g, 11.17 mmol) in methanol (50 ml) and chloroform (100 ml) was added to the reaction mixture and refluxed at 70 °C for 3 h. The product was purified using column chromatography using chloroform as the eluent. The product yield was 23% (2.17 g). ^{1}H NMR (400 MHz; $CDCl_3$; Me_4Si): 9.01 (8.77 (t, 8H), 8.11–7.84 (t, 12H), 7.30 (s, 4H), 4.21 (s, 4H), 3.33–0.86 (m, 22H). Elem. Anal. for $C_{56}H_{52}N_4O_2Br_2Zn$ Calc.: C, 64.79; H, 5.04; N, 5.39; O, 3.47. Found: C, 64.15; H, 4.88; N, 5.14; O, 3.48.

2.3.4. General polymerization method

Reaction monomers (0.5 mmol), $Pd(PPh_3)_4$ (1.5 mol%), and Aliquat 336 were dissolved in a mixture of toluene and an aqueous solution of 2 M K_2CO_3. The solution was refluxed for 72 h with vigorous stirring in a nitrogen atmosphere, and then the excess amount of bromobenzene, which was the end capper, was added and stirring continued for 12 h. The whole mixture was poured into methanol. The precipitate was filtered off, purified with acetone, hexane, and chloroform in a soxhlet.

2.3.5. PFPor

Red powder: 0.30 g (yield, 42.9%). ^{1}H NMR (400 MHz; $CDCl_3$; Me_4Si): 9.09 (br, 4H), 9.00 (br, 4H), 8.34 (br, 4H), 8.20–7.50 (br, 14H), 7.25 (br, 4H), 4.20 (br, 4H), 1–3 (76H, CH_2(subscript), CH_3(subscript)). Elem. Anal. for $C_{85}H_{92}N_4O_2Zn$ Calc.: C, 80.56; H, 7.32; N, 4.42; O, 2.53. Found: C, 80.50; H, 7.49; N, 4.05; O, 2.48.

2.3.6. PCPor

Red powder: 0.55 g (yield, 76.4%). ^{1}H NMR (400 MHz; $CDCl_3$; Me_4Si): 9.09 (br, 4H), 9.01 (br, 4H), 8.36 (br, 4H), 8.20–7.50 (br, 14H), 7.25 (br, 4H), 4.92 (br, 1H), 4.22 (br, 4H), 1–3 (76H, CH_2(subscript), CH_3(subscript)). Elem. Anal. for $C_{85}H_{93}N_5O_2Zn$ Calc.: C, 79.63; H, 7.31; N, 5.45; O, 2.50. Found: C, 79.71; H, 7.48; N, 5.30; O, 2.51.

3. Results and discussion

3.1. Synthesis and characterization

PFPor and PCPor were synthesized by a Suzuki coupling reaction, as shown in Scheme 1. The synthesized polymer

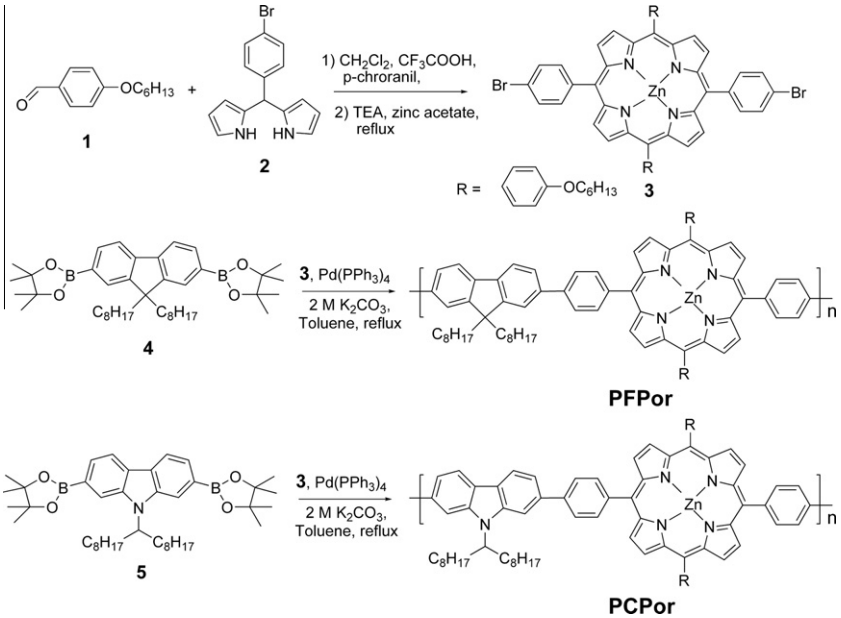

Scheme 1. The synthetic routes of PFPor and PCPor.

was refined by a soxhlet extraction in the order of methanol, acetone, and hexane, and the chloroform soluble fraction was recovered and dried under a reduced pressure at 50 °C. The ^{1}H NMR spectrum of the polymers were illustrated in Fig. 1. The two polymers had good solubilities in common organic solvents, such as chloroform, THF, toluene, chlorobenzene (CB), *o*-dichlorobenzene (*o*-DCB), etc. The number average molecular weight (M_n) of PFPor and PCPor were 19.7, 15.2 kg/mol and the weight average molecular weight (M_w) of them were 109.6, 36.2 kg/mol, and their PDI values were 5.56 and 2.38, respectively. Compared to PCPor, PFPor had a relatively high polydispersity (PDI) value. On considering that a high PDI value has a bad effect on electronic properties of conjugated polymers, it was estimated that the high PDI value of PFPor could be one cause that hinders its various optoelectronic properties.

As shown in Fig. 2, the polymers had decomposition temperatures (T_d) over 385 °C, which indicated that they had good thermal stability, making them applicable for use in polymer solar cells and other optoelectronic devices. The results of molecular weight measurements and thermal properties are shown in Table 1.

3.2. Optical and electrochemical properties

The UV–Vis absorption spectrum were measured in solution and film (Fig. 3a). PFPor and PCPor both exhibited a strong absorption peak at 428 nm and two weak absorption peaks at 550 and 591 nm in solution. In films, PFPor exhibited a strong absorption peak at 436 nm and two weak absorption peaks at 556 and 598 nm. Likewise, PCPor indicated a strong absorption peak at 435 nm and two weak absorption peaks at 556 and 598 nm.

In the case of films, both of the two polymers exhibited absorption peaks in about the same wavelength. The strong absorption observed at 436 and 435 nm were the Soret absorption bands of the porphyrin derivatives and the weak absorption observed at 556 and 598 nm were the Q-absorption bands of the porphyrin derivative as typical absorption peaks of zinc porphyrin compounds. Compared to the solution state, in film, the two polymers had broad Soret bands and Q-bands. Particularly, the intensity

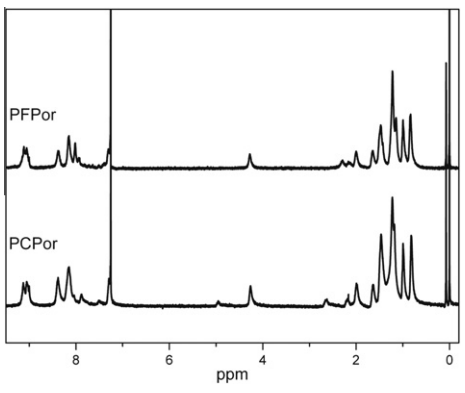

Fig. 1. ^{1}H NMR spectra of PFPor and PCPor.

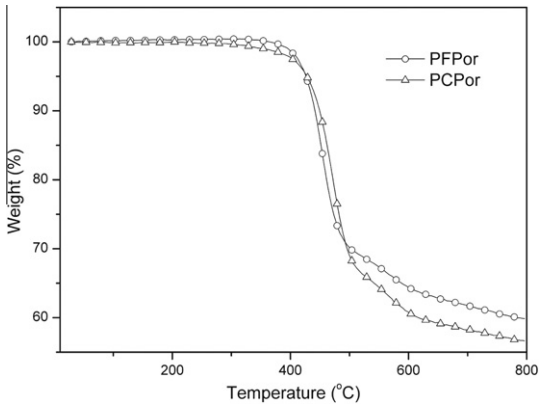

Fig. 2. TGA curves of PFPor and PCPor.

Table 1
Molecular weights and thermal properties.

Polymer	Yield (%)	M_n (kg/mol)	M_w (kg/mol)	PDI	T_d (°C)
PFPor	42.9	19.7	109.6	5.56	405
PCPor	76.4	15.2	36.2	2.38	385

Molecular weights and ploydispersity indexes determined by GPC in THF on the basis of polystyrene calibration.

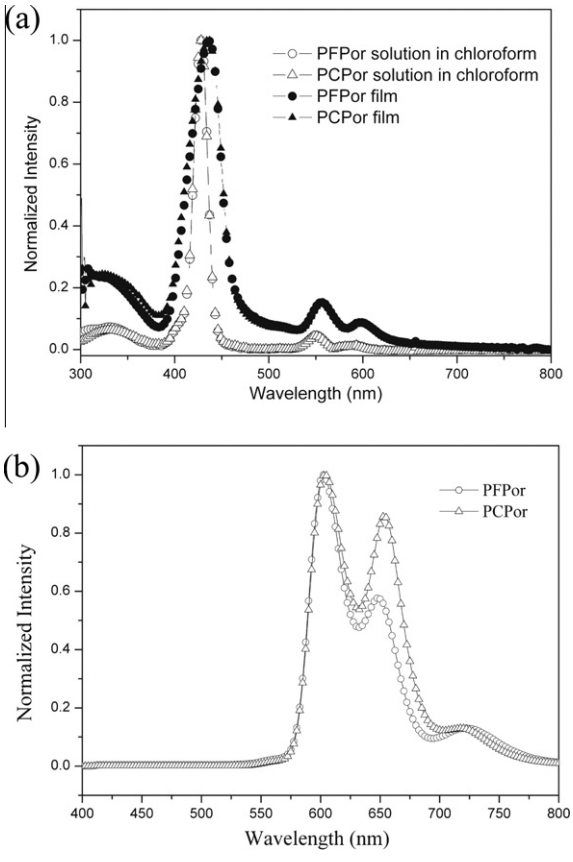

Fig. 3. Comparison of (a) UV–Vis absorption spectrum and (b) PL emission spectrum of PFPor and PCPor.

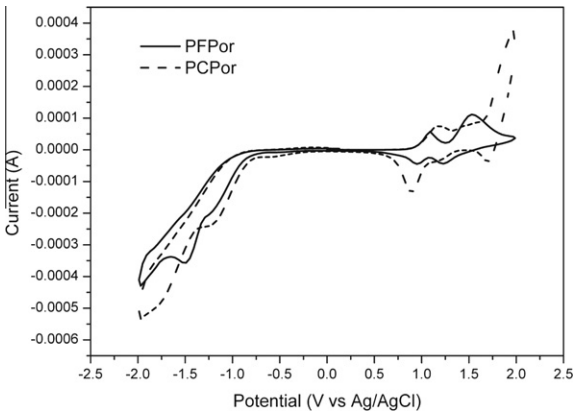

Fig. 4. Cyclic voltammograms of PFPor and PCPor recorded in 0.1 M Bu_4NPF_6/acetonitrile at a scan rate of 50 mV/s.

of the Q-bands increased. In addition, both Soret bands and Q-bands were red-shifted by about 8 nm. This originated from the improved intermolecular interaction between the polymer chains in the films. The optical band gaps were calculated through the onset value of the UV–Vis absorption spectrum in polymer films. The optical band gaps of PFPor and PCPor were 1.95 and 1.94 eV, respectively.

Fig. 3(b) depicts the photoluminescence (PL) spectra of PFPor and PCPor in solution. PFPor exhibited a maximum emission peak at 602 nm and another emission peak at 648 nm. Similar to PFPor, PCPor indicated a maximum emission peak at 604 nm and another strong emission peak at 653 nm. Considering that the zinc porphyrin compound exhibited two emission peaks at 600 and 650 nm, the emission peaks of the two polymers arose from the zinc porphyrin compound. Nevertheless, PCPor exhibited more red-shifted emission peaks than did PFPor. Additionally, the emission peak around 650 nm was more developed than PFPor [28,29]. It appeared that intramolecular interactions and energy transfer from electron donating units (fluorene or carbazole) to porphyrin were more effective in PCPor than in PFPor.

The electrochemical behavior of the copolymers was investigated using cyclic voltammetry (CV). The lowest unoccupied molecular orbital (LUMO) levels were calculated from the differences between the HOMO energy levels and the optical band-gaps, that were determined using the UV–Vis absorption onset values in the films. Fig. 4 shows the cyclic voltammograms of PFPor and PCPor. The electrochemically calculated energy HOMO levels of PFPor and PCPor were both −5.31 eV. Both of the polymers appeared very stable in the oxidative state. The LUMO levels of the polymers were −3.36 and −3.37 eV, respectively. The reason that the two polymers had low HOMO energy levels were that the electron donating materials, fluorene or carbazole, had low HOMO energy levels. Considering that the V_{OC} value is determined by the difference between the HOMO level of the donor polymer and the LUMO level of the acceptor, it is expected that PFPor and PCPor will

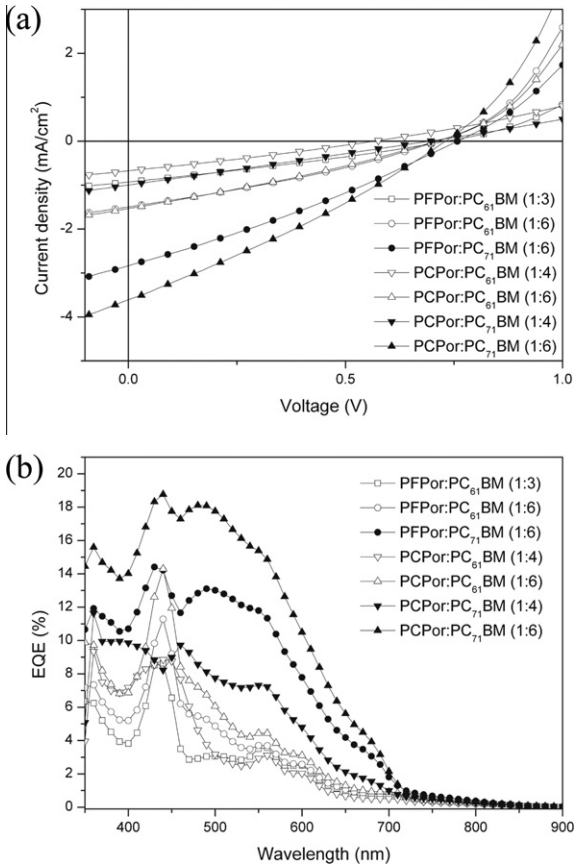

Fig. 5. Comparison of (a) J–V characteristics and (b) EQE data of bulk heterojunction photovoltaic devices based on PFPor or PCPor/PCBM.

Table 2
Optical, electrochemical data and energy levels of polymers.

Polymers	UV–Vis absorption spectrum			PL emission spectrum	E_g^{op} (eV)[b]	E_{onset}^{ox} (V)	Energy level (eV)	
	In $CHCl_3$	In film[a]		In $CHCl_3$			HOMO[c]	LUMO[d]
	λ_{max} (nm)	λ_{max} (nm)	λ_{onset} (nm)	λ_{max} (nm)				
PFPor	428*, 450, 493	436*, 556, 598	635	602, 648	1.95	0.92	−5.31	−3.36
PCPor	428*, 450, 493	436*, 556, 598	639	604, 653	1.94	0.92	−5.31	−3.37

[a] Spin-coated from a chloroform.
[b] Estimated from the onset of UV–Vis absorption data of the thin film.
[c] Calculated from the oxidation onset potentials under the assumption that the absolute energy level of Fc/Fc^+ was −4.8 eV below a vacuum.
[d] HOMO-Egop.
* Main absorption peak.

exhibit high V_{OC} values in photovoltaic devices. The optical and electrochemical data are summarized in Table 2.

3.3. Morphology analysis and photovoltaic studies

Bulk heterojunction solar cells using PFPor and PCPor as donor materials and PCBM as acceptor materials were fabricated with a structure of ITO/PEDOT:PSS/polymer:PCBM/BaF_2/Ba/Al. Two sorts of PCBM, $PC_{61}BM$ and $PC_{71}BM$, were introduced as acceptor materials in order to confirm the acceptor effect in the polymer/PCBM blend. The weight ratio between the donor polymer and PCBM were considered as a key factor that governed the photovoltaic property. Thus, typical active layer films were fabricated with weight ratios of one part donor polymer to six parts PCBM for effective development of p, n-channels between donor polymer chains, including bulky porphyrin compounds and PCBM. All the photovoltaic measurements were performed under 100 mW/cm^2 AM 1.5 sun illumination in ambient conditions.

A typical J–V curve and the external quantum efficiency (EQE) of PFPor and PCPor is presented in Fig. 5. When $PC_{61}BM$ was introduced as an acceptor, the PCEs of PFPor and PCPor were 0.32% and 0.31%, respectively. Although relatively good V_{OC} values, over 0.7 V, were observed, the PCE values were governed by the short circuit current density (J_{SC}) values as low as 1.5 mA/cm^2.

To confirm the acceptor effect in the polymer/PCBM blend, $PC_{71}BM$ was introduced instead of $PC_{61}BM$ as an acceptor. The PCE of the devices with PFPor/$PC_{71}BM$ and PCPor/$PC_{71}BM$ blend films as active layers were regularly 0.62% and 0.76%, respectively, in the device where 86 wt.% of the $PC_{71}BM$ was contained in the active layer (pol:$PC_{71}BM$ = 1:6, w/w).

Compared to devices introducing $PC_{61}BM$ as an acceptor material, photovoltaic devices adopting the polymer/$PC_{71}BM$ blend films had higher PCE values, which depended on the differences of the J_{SC} values. These differences originated from absorption property between acceptors, $PC_{61}BM$ and $PC_{71}BM$, and film morphology. It is well known that $PC_{71}BM$ has a stronger UV–Vis absorption property than does $PC_{61}BM$ in the visible region, especially around 500 nm [30]. As shown in Fig. 5b, devices where $PC_{71}BM$ was introduced as an acceptor had increased EQE around the 500 nm wavelength region.

In addition, as shown in Fig. 6, the polymer/$PC_{71}BM$ blend films indicated more detailed p, n-channels than the polymer/$PC_{61}BM$ blend films. After considering that well developed p, n-channels of active layers have a crucial effect on J_{SC} values and fill factor (FF), it was thought that the differences in morphologies between the polymer/PCBM blend films was an important factor for the improvement of the PCE value.

Nevertheless, both of polymers had relatively low PCE values of below 1.0%. One reason of the low PCE values for these polymers were their high LUMO levels, since a large difference of LUMO energy levels between a donor and acceptor allows for increased energy loss in photovoltaic devices [31,32]. Another reason was the band gap energy. The optical band gap energies of PFPor and PCPor

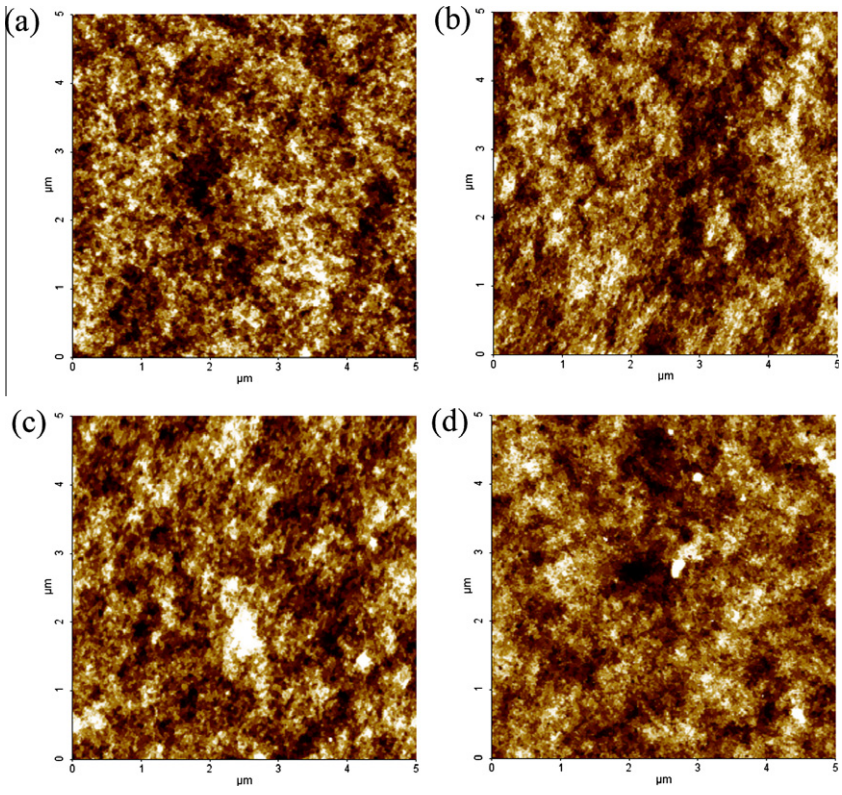

Fig. 6. AFM images of active layer films: (a) PFPor/$PC_{61}BM$, (b) PFPor/$PC_{71}BM$, (c) PCPor/$PC_{61}BM$, (d) PCPor/$PC_{71}BM$ blend films.

Table 3
Summary of photovoltaic characteristics of devices.

Active layer (w/w)		Weight ratio (P:A, w/w)	V_{OC} (V)	J_{SC} (mA/cm^2)	FF	PCE (%)
Polymer (P)	Acceptor (A)					
PFPor	$PC_{61}BM$	1:3	0.75	0.9	0.28	0.19
		1:6	0.71	1.5	0.30	0.32
	$PC_{71}BM$	1:6	0.75	2.8	0.29	0.62
PCPor	$PC_{61}BM$	1:4	0.70	1.3	0.26	0.25
		1:6	0.71	1.5	0.29	0.31
	$PC_{71}BM$	1:4	0.70	2.4	0.26	0.43
		1:6	0.73	3.6	0.29	0.76

were not low enough to absorb photons in the long wavelength region. The other reason was the narrow absorption range. Although they had absorption onsets around 640 nm, the absorption spectra were not continuous over all of the absorption range.

Therefore, in order to develop efficient photovoltaic polymer materials that include a porphyrin compound, polymer materials designed to improve their absorption property by inducing effective intramolecular charge transfer between electron donors and electron acceptors have to be designed and synthesized through molecular tailing [33]. In addition, well-balanced energy levels by introducing various functional groups have to be considered. The photovoltaic properties of PFPor and PCPor are presented in Table 3.

4. Conclusion

In summary, PFPor and PCPor, which are based on porphyrin, were successfully synthesized through the Suzuki coupling reaction for OPVs. They exhibited good thermal stability and optical band gaps as low as 1.95 eV. PCPor exhibited a PCE value of 0.76% (V_{OC} = 0.73 V, J_{SC} = 3.6 mA/cm^2, FF = 0.29) in the device where 86 wt.% of the $PC_{71}BM$ was contained in the active layer (pol:$PC_{71}BM$ = 1:6, w/w). Although the two polymers did not exhibit very high PCEs, if absorption properties of these materials reinforce by enlarging a conjugation length and improving charge transferred property through adopting efficient spacer materials in polymer backbones, it is expected that new high performance organic photovoltaic materials will be developed.

Acknowledgements

This research was supported by a grant from the National Research Foundation of Korea Grant funded by the Korean Government(MEST) (NRF-2009-C1AAA001-2009-0093526), and the New and Renewable Energy R&D program (2008-N-PV08-02) under the Korea Ministry of Knowledge Economy (MKE).

References

[1] Krebs FC, Fyenbo J, Jørgensen M. Product integration of compact roll-to-roll processed polymer solar cell modules: methods and manufacture using flexographic printing, slot-die coating and rotary screen printing. J Mater Chem 2010;20:8994–9001.
[2] Krebs FC, Tromholt T, Jørgensen M. Upscaling of polymer solar cell fabrication using full roll-to-roll processing. Nanoscale 2010;2:873–86.
[3] Krebs FC. Polymer solar cell modules prepared using roll-to-roll methods: knife-over-edge coating, slot-die coating and screen printing. Sol Energy Mater Sol Cells 2009;93:465–75.
[4] Krebs FC. Fabrication and processing of polymer solar cells: a review of printing and coating techniques. Sol Energy Mater Sol Cells 2009;93:394–412.
[5] Krebs FC, Gevorgyan SA, Alstrup J. A roll-to-roll process to flexible polymer solar cells: model studies, manufacture and operational stability studies. J Mater Chem 2009;19:5442–51.
[6] Bronstein H, Chen Z, Ashraf RS, Zhang W, Du J, Durrant JR, et al. Thieno[3,2-b]thiophene-diketopyrrolopyrrole-containing polymers for high-performance organic field-effect transistors and organic photovoltaic devices. J Am Chem Soc 2011;133:3272–5.
[7] Ong KH, Lim SL, Tan HS, Wong HK, Li J, Ma Z, et al. A versatile low bandgap polymer for air-stable, high-mobility field-effect transistors and efficient polymer solar cells. Adv Mater 2011;23:1409–13.
[8] Zhao G, He Y, He C, Fan H, Zhao Y, Li Y. Photovoltaic properties of poly-(benzothiadiazole-thiophene-co-bithiophene) as donor in polymer solar cells. Sol Energy Mater Sol Cells 2011;95:704–11.
[9] Hou Q, Xu X, Guo T, Zeng X, Luo S, Yang L. Synthesis and photovoltaic properties of fluorene-based copolymers with narrow band-gap units on the side chain. Euro Polym J 2010;46:2365–71.
[10] Huo L, Hou J, Zhang S, Chen HY, Yang Y. A polybenzo[1,2-b:4,5-b′]dithiophene derivative with deep homo level and its application in high-performance polymer solar cells. Angew Chem Int Ed 2010;49:1500–3.
[11] Zhang Y, Hau SK, Yip HL, Sun Y, Acton O, Jen AKY. Efficient polymer solar cells based on the copolymers of benzodithiophene and thienopyrroledione. Chem Mater 2010;22:2696–8.
[12] Lee JY, Shin WS, Haw JR, Moon DK. Low band-gap polymers based on quinoxaline derivatives and fused thiophene as donor materials for high efficiency bulk-heterojunction photovoltaic cells. J Mater Chem 2009;19:4938–45.
[13] Cheng YJ, Yang SH, Hsu CS. Synthesis of conjugated polymers for organic solar cell applications. Chem Rev 2009;109:5868–923.
[14] Bundgaard E, Krebs FC. Low band gap polymers for organic photovoltaics. Sol Energy Mater Sol Cells 2007;91:954–85.
[15] Hagemann O, Jørgensen M, Krebs FC. Synthesis of an all-in-one molecule (for organic solar cells). J Org Chem 2006;71:5546–59.
[16] Krebs FC, Spanggaard H. Antibatic photovoltaic response in zincporphyrin-linked oligothiophenes. Sol Energy Mater Sol Cells 2005;88:363–75.
[17] Nielsen KT, Spanggaard H, Krebs FC. Synthesis, light harvesting, and energy transfer properties of a zinc porphyrin linked poly(phenyleneethynylene). Macromolecules 2005;38:1180–9.
[18] Kumar S, Manickam M. Nitration of triphenylene discotics: synthesis of mononitro-, dinitro- and trinitro-hexaalkoxytriphenylenes. Mol Cryst Liq Cryst 1998;309:291–5.
[19] Boden N, Bushby RJ, Cammidge AN, Duckworth S, Headdock G. A-halogenation of triphenylene-based discotic liquid crystals: towards a chiral nucleus. J Mater Chem 1997;7:601–5.
[20] Huang X, Zhu C, Zhang S, Li W, Guo Y, Zhan X, et al. Porphyrin-dithienothiophene π-conjugated copolymers: synthesis and their applications in field-effect transistors and solar cells. Macromolecules 2008;41:6895–902.
[21] Hasobe T, Sandanayaka ASD, Wada T, Araki Y. Fullerene-encapsulated porphyrin hexagonal nanorods. An anisotropic donor–acceptor composite for efficient photoinduced electron transfer and light energy conversion. Chem Commun 2008;29: 3372–4.
[22] Hasobe T, Imahori H, Kamat PV, Ahn TK, Kim SK, Kim D, et al. Photovoltaic cells using composite nanoclusters of porphyrins and fullerenes with gold nanoparticles. J Am Chem Soc 2005;127: 1216–28.
[23] Xiang N, Liu Y, Zhou W, Huang H, Guo X, Tan Z, et al. Synthesis and characterization of porphyrin-terthiophene and oligothiophene π-conjugated copolymers for polymer solar cells. Euro Polym J 2010;46:1084–92.
[24] Temelli B, Unaleroglu C. A novel method for the synthesis of dipyrromethanes by metal triflate catalysis. Tetrahedron 2006;62:10130–5.
[25] Kroon R, Lenes M, Hummelen JC, Blom PWM, de Boer B. Small bandgap polymers for organic solar cells (polymer material development in the last 5 years). Polym Rev 2008;48:531–82.
[26] Lee JY, Choi MH, Moon DK, Haw JR. Synthesis of fluorene- and anthracene-based π-conjugated polymers and dependence of emission range and luminous efficiency on molecular weight. J Ind Eng Chem 2010;16:395–400.

[27] Blouin N, Michaud A, Leclerc M. A low-bandgap poly(2,7-carbazole) derivative for use in high-performance solar cells. Adv Mater 2007;19:2295–300.
[28] Song KW, Lee JY, Heo SW, Moon DK. Synthesis and characterization of a fluorene–quinoxaline copolymer for light-emitting applications. J Nanosci Nanotechnol 2010;10:99–105.
[29] Lee JY, Kwon YJ, Woo JW, Moon DK. Synthesis and characterization of fluorine, thiophene-based π-conjugated polymers using coupling reaction. J Ind Eng Chem 2008;14:810–7.
[30] Peet J, Kim JY, Coates NE, Ma WL, Moses D, Heeger AJ, et al. Efficiency enhancement in low-bandgap polymer solar cells by processing with alkane dithiols. Nat Mater 2007;7:497–500.
[31] Blouin N, Michaud A, Gendron D, Wakim S, Blair E, Neagu-Plesu R, et al. Toward a rational design of poly(2,7-carbazole) derivatives for solar cells. J Am Chem Soc 2008;130:732–42.
[32] Scharber MC, Mühlbacher D, Koppe M, Denk P, Waldauf C, Heeger AJ, et al. Design rules for donors in bulk-heterojunction solar cells – towards 10% energy-conversion efficiency. Adv Mater 2006;18:789–94.
[33] Roncali J. Synthetic principles for bandgap control in linear π-conjugated systems. Chem Rev 1997;97:173–205.